Laser wavemeter with solid Fizeau wedge interferometer

Christopher Reiser and R. B. Lopert

A Fizeau wavemeter using a solid Fizeau wedge interferometer that is suitable for determining the wavelength of pulsed or cw laser light has been modeled and investigated experimentally. Accuracy of a few parts in 10^6 over a wide wavelength range can be achieved with careful design. Experimental accuracy of 2 parts in 10^6 was demonstrated over a range of 40 nm.

I. Introduction

Of paramount importance in uses of the laser such as lidar, laser isotope separation, and laser spectroscopy is knowing the wavelength of the light produced by a tunable system. As Snyder[1–5] and others[6–10] have demonstrated, very accurate determinations of laser wavelength can be made with a vacuum-spaced Fizeau wedge interferometer. That instrument, whose basic optical design is shown in Fig. 1(a), can measure both pulsed and cw sources.

The operation of a vacuum-spaced Fizeau wedge interferometer requires that the Fizeau wedge be enclosed in a container that maintains a vacuum, a requirement that makes construction of the instrument difficult. Placing the Fizeau wedge in a vacuum container and sending light into and out of the wedge via a window cause errors to be introduced by the dispersion effects that occur in the window. Various techniques have been suggested[6,8,10,11] for easing the vacuum requirements and improving the accuracy of the Fizeau wavemeter. These include filling the interferometer with a calibrated amount of gas,[6] bringing the detector array into close proximity to the interferometer,[6,10] or using multiple interferometers.[9,12] Such systems may eliminate the vacuum requirement but still result in instruments that are difficult and expensive to construct.

Considerable simplification of the optical train of the wavemeter can be realized if the interferometer is constructed from a solid optical material such as BK7 glass or fused silica. As shown in Fig. 1(b), this eliminates both the vacuum system that encloses the interferometer and the compensating plate that is used to cancel chromatic effects caused by the vacuum container window. The price for this simplification lies in effects caused by dispersion of the solid Fizeau interferometer (SFI).

As shown below by geometrical modeling and ray-tracing techniques, the effects of SFI dispersion can be unraveled so that accurate wavelength determinations can be made. Furthermore, in the first laboratory demonstration of an SFI instrument, we show that good performance can be attained in a practical system.

II. Principles of Operation

Operation of a wavemeter with an SFI is similar to the operation of a vacuum-spaced Fizeau wedge instrument as described by Snyder[5] [see Fig. 1(a)]. Incoming light is focused through a filtering pinhole, expands, and is collimated by an off-axis parabolic mirror. The wavefront at plane S has very low curvature[6,11] as it travels toward the interferometer. A portion of the light reflects from the front interferometer surface, while a nearly equal portion reflects from the rear interferometer surface. The two reflected beams travel toward the photodiode array at slightly different angles as determined by the angle of the Fizeau wedge. The cylindrical lens focuses these two beams onto the photodiode array, where an interference pattern is generated by the interaction of the two beams from the Fizeau wedge. By measuring the period and phase of the pattern with the photodiode array it is possible to estimate the wavelength of the incident light.

When an SFI is used, no vacuum container is required. This eliminates the vacuum chamber window, the front wedge plate, and the compensating plate from the optical train between surface S and the detector, as seen in Fig. 1(b). In this case, the reflection from the front SFI surface reaches the cylindrical lens

Christopher Reiser is with Sandia National Laboratories, Albuquerque, New Mexico 87185-5800, and R. B. Lopert is with Cherokee Data Systems, 1800 South Flatiron Court, Boulder, Colorado 80301.
Received 28 December 1987.
0003-6935/88/173656-05$02.00/0.

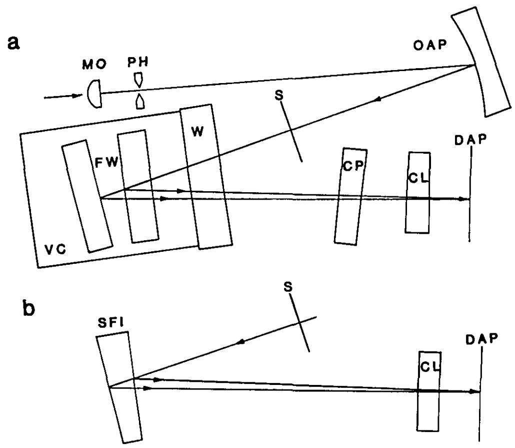

Fig. 1. (a) Typical vacuum wedge wavemeter optical layout similar to Ref. 5; (b) SFI wavemeter layout from plane S onward: MO, microscope objective; PH, pinhole; OAP, off-axis paraboloid mirror; W, vacuum container window; FW, Fizeau wedge; VC, vacuum container; CP, compensating plate; CL, cylindrical lens; DAP, detector array plane.

without intersecting any optics. The reflection from the rear SFI surface refracts into and out of the SFI and becomes slightly sheared (laterally displaced) from the front reflection. At a distance determined by the exit angles of the reflections, the two rays meet at a zero shear[3,8] line.

To minimize the effects of wavefront errors in the collimated beam, the photodiode array should be placed along the zero shear line. The interference that occurs at a given point on this line is caused by two rays from the wedge that both originate from the same point in the input plane S (see Fig. 2). Placing the photodiode array at the zero shear line minimizes lateral shear of the wavefronts and simplifies analysis of the instrument.

At the detector, the interference forms a normalized intensity pattern $I(x)$ so that[5]

$$I(x) = \left\{1 + \cos\left[\frac{2\pi(x + P_0/S)}{\Lambda}\right]\right\}\Big/2, \tag{1}$$

where x is the direction along the photodiode array, Λ is the fringe period given by

$$\Lambda = \lambda/n(\lambda)S = l/S. \tag{2}$$

Here λ is the vacuum wavelength, $l = \lambda/n(\lambda)$ is the wavelength inside the SFI, and $n(\lambda)$ is the index of refraction of the SFI at λ. In Eq. (1), P_0 is the physical path difference for rays that strike the detector array at $x = 0$. Constant S, related to the angle of the SFI, is the change in physical path difference P per change in x:

$$S = \Delta P/\Delta x \approx 2\tan\alpha \sim 2\alpha, \tag{3}$$

where α is the physical angle of the wedge in the SFI.

One problem that can be gleaned from Fig. 2 is that P_0 is not constant for media with dispersion, since the internal angle of the rays that traverse the SFI changes with $n(\lambda)$. Blue rays will not trace precisely the same path as red rays, giving rise to an error that varies

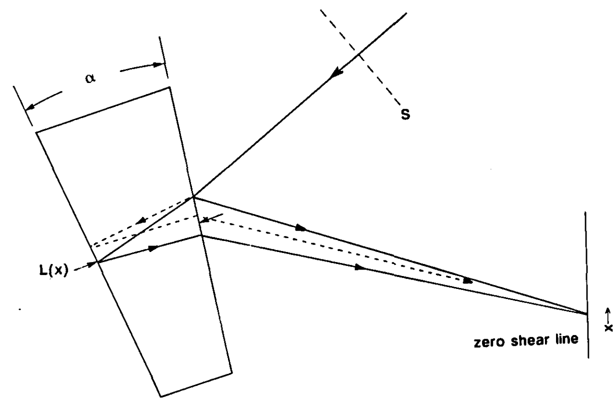

Fig. 2. Closeup of rays in the SFI. Path followed by a blue ray is indicated with a dashed line.

systematically with $n(\lambda)$. We will make a simple correction for this effect,

$$P_0 = L + [n(\lambda) - n_{\mathrm{reff}}]A, \tag{4}$$

where L is a constant for all wavelengths, n_{reff} is a reference index, and A is a constant determined empirically. The net effect of Eq. (4) is to correct a chromatic aberration caused by dispersion in the SFI medium that results in a translation of the fringe pattern in the x direction.

Determining the wavelength from fringe data is a four-step process. Once the wavemeter is calibrated, that is, the values of L, A, S, D, and n_{reff} are found, the first wavelength estimate can be made from the measured fringe spacing Λ via

$$\lambda_1 = \Lambda n(\lambda_g)S \tag{5}$$

$$\approx \Lambda n_{\mathrm{calc}}(\lambda_g)S + D, \tag{6}$$

where λ_g is an initial guess of the wavelength. Note that the calibration constant D compensates for discrepancies between the actual index $n(\lambda_1)$ of the SFI material and the calculated index $n_{\mathrm{calc}}(\lambda_1)$. Next, the physical path difference P_m at a fringe minimum close to $x = 0$ is calculated. Since an integer number of wavelengths fit into this P_m, the integer m is found from

$$P_m = P_0 + Sx_m = m\lambda_1/n_{\mathrm{calc}}(\lambda_1). \tag{7}$$

The exact wavelength λ_2 is approximated by

$$\lambda_2 = n_{\mathrm{calc}}(\lambda_1)\,\frac{P_m}{m} \tag{8}$$

and finally calculated via

$$\lambda_3 = n_{\mathrm{calc}}(\lambda_2)\,\frac{P_m}{m}\,. \tag{9}$$

III. Simulations

Thanks to the simplicity of the SFI wavemeter design, it is a straightforward task to solve the geometry for tracing rays from plane S to the detector plane. Using a simple computer program, the optical path difference O between the two interfering rays was calculated for two thicknesses of the SFI for BK7 glass and for fused silica. The index of refraction used in the calculations was taken from the literature[13] for fused silica and from the manufacturer's catalog[14] for BK7.

In Fig. 3 a calculated parameter related to P_0 is plotted against index. This parameter is the relative optical path difference given by $T = O[n(500\ \text{nm})] - O[n(\lambda)] \approx n(500\ \text{nm})P_0[n(500\ \text{nm})] - n(\lambda)P_0[n(\lambda)]$. In this calculation, the incoming rays strike the SFI at 11°, and the detector array is 30 cm from the SFI. If Eq. (4) is a valid model for the SFI, the calculated T should fall on a straight line, as it does for wavelengths between ~450 and 1000 nm. Departures from linearity below 450 nm imply that the SFI wavemeter will exhibit increasing error beyond this point.

Of practical concern is the location of the zero shear plane. Placing the detector at this plane minimizes the sensitivity of the instrument to phase imperfections at plane S.[3,8] Calculated positions of the zero shear line are shown in Fig. 4 for a variety of geometries. The data show that the overall size of the SFI instrument will be in the 20-cm range.

More complete modeling of the SFI system was accomplished using a computer program written explicitly for tracing rays through a Fizeau wavemeter. For a given wavemeter design, the program calculates the optical path difference for rays striking the detector array at various points on the array. From these data, the detector response is determined, and values for the optical path difference at a fringe minimum near the beginning of the photodiode array and Λ are found. This procedure is done for many wavelengths, after which the design under simulation can be calibrated and run as if it were a real system.

Calibration of the design under simulation was done in several steps. A group of 6–8 wavelengths spaced 0.1 nm apart was used to find a value for P_0 by Snyder's method.[1] Over this range, dispersion is a small effect, and n_{reff} is taken to be the index of the average wavelength of the set. Values for S and D are found by a least-squares fitting of the observed fringe periods Λ to the $n_{\text{calc}}(\lambda)$. The chromatic constant A is found by using a second set of 6–8 wavelengths spaced at least 20 nm from the first set to calibrate the wavemeter a second time. The difference is values of P_0 between the two sets is used to calculate a value for A.

We have simulated a total of four wavemeter designs. All designs featured rays incident on the SFI at 11°, internal SFI angle of 3 min, and a detector assembly including BK7 cylindrical lens located ~30 cm from the SFI. Both BK7 and fused silica were investigated, each at two thicknesses, 0.9935 and 0.6896 mm. The first set of calibration wavelengths was centered at 900.3 nm and the second set at 600.3 nm. Results from the simulated calibrations are shown in Table I. It must be noted that the thick BK7 case did not successfully calibrate, and thus it is omitted from the table.

Since the critical step in calculating the wavelength determines the order number m per Eq. (7), the λ_1 calculated from Eq. (6) must be accurate to better than 0.5 parts in m for all wavelengths. In practice, the requirement is barely met.[5] In the simulations, we found that the difference between λ_1 and the actual wavelength stayed below the $10^{-5}\lambda$ level over the range of 500–900 nm (see Fig. 5). This indicates that for a thin SFI, λ_1 should be sufficiently accurate to deter-

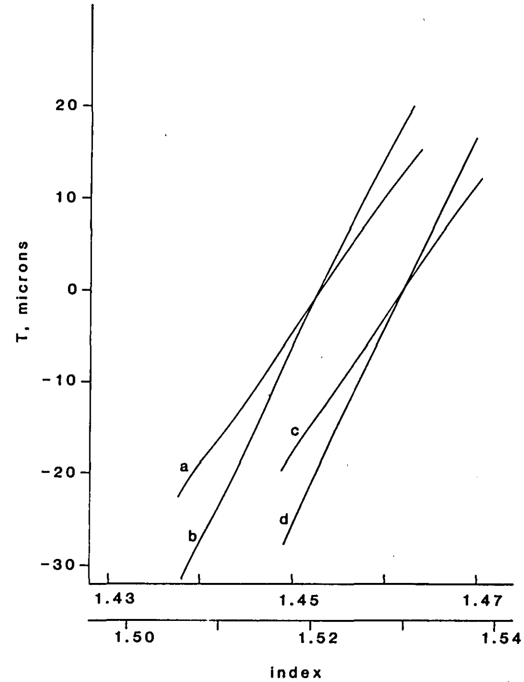

Fig. 3. Calculated parameter T vs index of SFI for (a) 0.6-mm BK7, (b) 0.9-mm BK7, (c) 0.6-mm fused silica, (d) 0.9-mm fused silica. Note separate scales for index: lower for BK7, upper for fused silica.

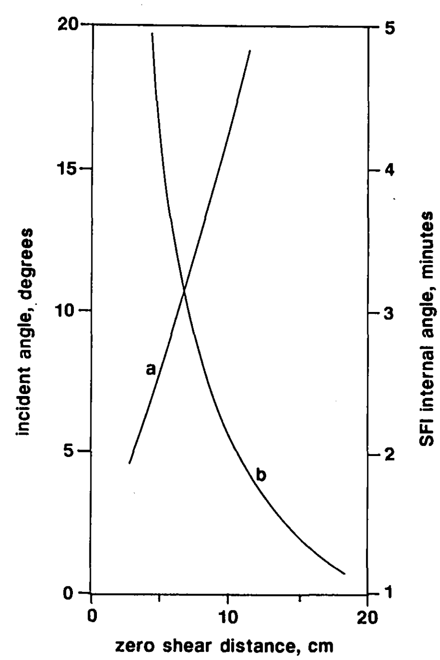

Fig. 4. Calculated zero shear distance for 0.6896-mm fused silica SFI for (a) 3-min wedge, various incident angles (left axis), (b) 11° incident angle, various wedge angles (right axis).

Table I. Calibration Constants from Simulations (First Three Entries) and Experiment (Last Entry)

Material	Thickness (mm)	L(Å)	A(Å)	S(Å/pixel)	D(Å)	$-n_{\mathrm{reff}}$
BK7	0.6896	13412430.0	140359.0	451.071	−1.387	1.5090018
Silica	0.6896	13403825.0	158374.0	450.780	−1.350	1.4517539
Silica	0.9935	19978693.0	238008.0	450.780	−1.350	1.4517539
Silica	0.99	19914536.0	42235.0	450.904	−2.4539	1.4576191

mine the order m unambiguously by Eq. (7) over a fairly wide spectral range.

The modeling program predicts the errors in the wavelength readings that would be expected of a real unit. These are shown in Fig. 6 for the various SFI designs. It can be seen that fused silica interferometers fared somewhat better than BK7, presumably because it has lower dispersion. Also, the thin fused silica interferometer behaved slightly better than its thick counterpart, implying that the simple corrections built into Eqs. (4) and (6) better represent the actual behavior of the thin system.

A source of error that the program does not calculate is the effect of temperature changes on the wavemeter readings. We can estimate the magnitude of this kind of error by using Eq. (9) and typical values for the variables:

$$\partial\lambda_3/\partial T = \frac{\partial P_m}{\partial T}\frac{n_{\mathrm{calc}}(\lambda_2)}{m} + \frac{\partial n(\lambda_2)}{\partial T}\frac{P_m}{m}. \tag{10}$$

For a fused silica SFI that is 0.6 mm thick, $m = 4000$, $n(\lambda) = 1.46$, the coefficient of thermal expansion[15] is $0.5 \times 10^{-6}\,{}^\circ\mathrm{C}^{-1}$, and the temperature coefficient of the index[13] is $11 \times 10^{-6}\,{}^\circ\mathrm{C}^{-1}$. Using these numbers, we find

$$\delta\lambda_3 \approx (1.15 \times 10^{-5}\lambda)\delta T \tag{11}$$

for λ in angstroms and δT in degrees Celsius. To maintain temperature effects to below the 10^{-6} level, regulation to better than 0.1°C would be necessary. This is more stringent than the vacuum-spaced design for which the $\partial n(\lambda_2)/\partial T$ term of Eq. (10) can be ignored.

IV. Experimental

Investigations of an SFI wavemeter in the laboratory began by removing the vacuum wedge assembly and the compensating plate from a Lasertechnics model 100 Fizeau wavemeter. A fused silica SFI with a 3-min wedge, having a thickness of 0.9 mm, was mounted in the same position as the vacuum wedge of the original unit. This configuration conforms closely to one simulated by the modeling program.

Light from a Coherent model 599 single-mode dye laser actively stabilized to an external reference cavity was injected into the wavemeter. As the laser was tuned across the rhodamine 6G curve in discrete jumps, its wavelength was determined to ±0.0001 nm by a traveling Michelson wavemeter referenced to a stabilized He–Ne laser.[16] At each wavelength, a single scan of the photodiode array was digitized and recorded for later analysis.

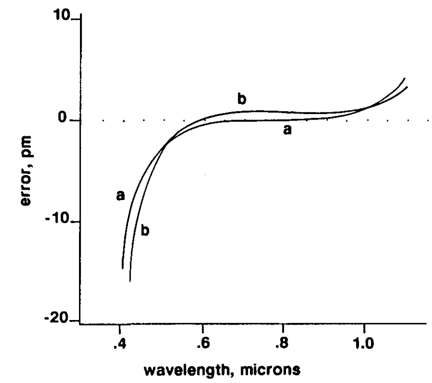

Fig. 5. Calculated errors (λ_1 − true wavelength) for 0.68-mm thick 3-min wedge SFI made from (a) fused silica and (b) BK7.

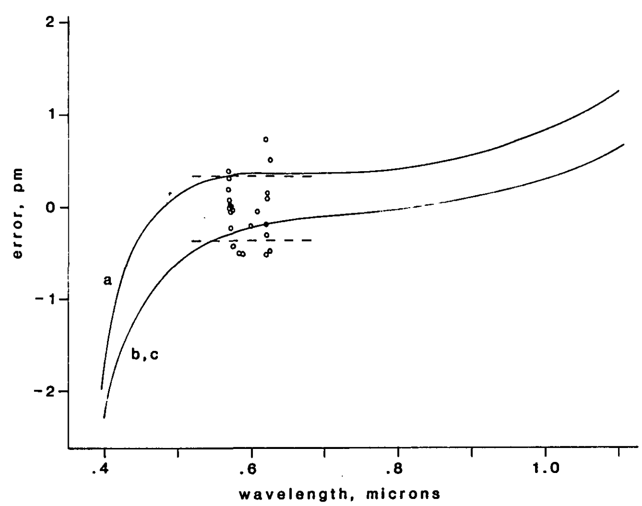

Fig. 6. Calculated chromatic errors for a 3-min wedge SFI simulated wavemeter performance (λ_3 − true wavelength) for (a) 0.68-mm BK7, (b) 0.68-mm fused silica, and (c) 0.99-mm fused silica. Chromatic errors for experimental SFI performance are shown as dots; 67% confidence interval (1σ) is shown as dashed lines.

A program derived from the modeling program was used to read and analyze the recorded fringe data. This program used Snyder's digital filter technique[17] to determine the fringe period and phase of each recorded fringe instead of simulating the detector array response. The two sets of wavelengths required by the calibration procedure were taken from opposite ends of the dye gain curve. In all other respects its operation was identical to the modeling program. It should be noted that the filter technique of Ref. 17 renders the statistical average fringe period Λ used in Eq. (6).

This technique effectively smooths out local fluctuations in the fringe period caused by local index inhomogeneities in the SFI.

Results of the calibration of the unit are shown in Table I. The calibration values compare well to the simulation.

Errors in the wavelength readings are depicted in Fig. 6 for 22 wavelengths. The average error is -0.00003 nm with a 1σ value of 0.00034 nm. This implies that the 99% confidence limit for a single-shot determination is $\sim$2 parts in 10^6 over the 40-nm range of the experiment. This is $\sim$5 times worse than that claimed by investigators[1,5,9,11] of vacuum-spaced interferometer systems.

The major reason for the degraded performance of the SFI instrument relative to the vacuum-spaced interferometer unit lies in our inability to calculate the index to better than the sixth decimal place or so. Calculation of the index with published formulas disagrees with the measured index[13] by $\sim$1 or 2 parts in 10^6. Such an error would give rise to an error in λ_3 of exactly the same magnitude. Also, although the wavemeter unit used in these experiments had long-term active temperature stabilization to 0.5°C, over the duration of the experiments a drift of 0.1°C could have reasonably occurred, giving rise to a systematic effect of the order of 10^{-6}.

V. Conclusions

Constructing a Fizeau wavemeter with a solid wedge, rather than a vacuum-space wedge, can simplify its design with only a slight decrease in accuracy. While calibration of the unit is more involved than with a vacuum-spaced interferometer, the overall cost of the system is decidedly lower. Either fused silica or BK7 is a reasonable choice of material for the SFI; fortuitously, the index of refraction of both materials can be calculated to high precision. Good temperature regulation of the SFI must be maintained for the system to attain a performance that is limited primarily by detector noise and the accuracy of calculating $n(\lambda)$. Overall, SFI offers a simple low cost solution to precision wavelength measurement of cw or pulsed laser light.

C. Reiser thanks Peter Esherick for the generous donation of rhodamine 6G photons.

This work was performed at Sandia National Laboratories, supported by the U.S. Department of Energy under contract DE-AC04-76DP00789.

References

1. J. J. Snyder, "Compact Static Wavelength Meter for Both Pulsed and CW Lasers," Sov. J. Quantum Electron. **8**, 959 (1978).
2. J. J. Snyder, "Fizeau Wavelength Meters," in *Laser Spectroscopy III*, J. L. Hall and J. L. Carlsten, Eds. (Springer-Verlag, New York, 1977), p. 419.
3. J. J. Snyder, "Fizeau Wavemeter," Proc. Soc. Photo-Opt. Instrum. Eng. **288**, 258 (1981).
4. J. J. Snyder, "Laser Wavelength Meters," Laser Focus **18**, 55 (May 1982).
5. M. B. Morris, T. J. McIlrath, and J. J. Snyder, "Fizeau Wavemeter for Pulsed Laser Wavelength Measurement," Appl. Opt. **23**, 3862 (1984).
6. J. L. Gardner, "Compact Fizeau Wavemeter," App. Opt. **24**, 3570 (1985).
7. L. J. Cotnoir, T. D. Wilkerson, M. Dombrowski, R. H. Kagann, C. L. Korb, G. K. Schwemmer, and H. Walden, "A Wavemeter for Use with a Line-Narrowed Alexandrite Laser in Differential Absorption Lidar," in *Technical Digest, Topical Meeting on Tunable Solid-State Lasers* (Optical Society of America, Washington, DC, 1985), paper FC5.
8. C. K. Miller, "Wavelength Meter for Pulsed Laser Applications," Sandia National Laboratories Report SAND81-0310 (Mar. 1982).
9. L.-S. Lee and A. L. Schawlow, "Multiple-Wedge Wavemeter for Pulsed Lasers," Opt. Lett. **6**, 610 (1981).
10. D. F. Gray, K. A. Smith, and F. B. Dunning, "Simple Compact Fizeau Wavemeter," Appl. Opt. **25**, 1339 (1986).
11. J. L. Gardner, "Wavefront Curvature Compensation in a Fizeau Wavemeter," Appl. Opt. **25**, 3799 (1986).
12. N. Konishi, T. Suzuki, Y. Taira, H. Kato, and T. Kasuya, "High Precision Wavelength Meter with Fabry-Perot Optics," Appl. Phys. **25**, 311 (1981).
13. I. H. Malitson, "Interspecimen Comparison of the Refractive Index of Fused Silica," J. Opt. Soc. Am. **55**, 1205 (1965).
14. *Optical Glass Technical Data* (Hoya Corp., Tokyo).
15. *Handbook of Optics*, W. G. Driscoll and W. Vaughan, Eds. (McGraw-Hill, New York, 1978).
16. P. Esherick and A. Owyoung, "High Resolution Stimulated Raman Spectroscopy," in *Advances in Infrared and Raman Spectroscopy*, R. J. Clark and R. E. Hester, Eds. (Heyden, London, 1982), Vol. 9, Chap. 3, pp. 130–187.
17. J. J. Snyder, "Algorithm for Fast Digital Analysis of Interference Fringes," Appl. Opt. **19**, 1223 (1980).